X-ray thin-film measurement techniques

VIII. Detectors and series summary

Shintaro Kobayashi* and Katsuhiko Inaba*

1. Introduction

The various XRD techniques as the characterization tools for thin film samples have been presented in this series of "X-ray thin-film measurement technique" lecture course. There has heretofore been remarkable progress with detectors equipped with XRD apparatus. In this lecture, some explanation of the features and functions of 1-dimensional (1D)/2-dimensional (2D) detectors should be presented before summarizing this technical lecture course.

2. Detectors for XRD system

As has been shown in first lecture of the series(1), an X-ray diffractometer system for thin film characterization is composed of 5 parts:

1. X-ray source
2. Incident optical system
3. Goniometer
4. Receiving optical system
5. Detection section

Scintillation counters and proportional counters are the most popular detectors for XRD systems and they are regarded as 0-dimensional (0D) detectors (or point detectors) because they do not have position information on the surface of the detecting components. Recently, however, detectors equipped with many detector-elements on its detection area have also come into general use in laboratory equipment. They are referred to as 1D or 2D detectors used for the high speed measurement. The functions and features of these detectors can be seen in references (2)~(5).

The variation of typical detectors available with the SmartLab system is shown in Fig. 1.

2.1. 0D Detector

The scintillation counter (SC) is mainly used for the SmartLab system because of its good sensitivity, low noise level and easy handling, etc. This detector can measure the count-rate from 0.1 to several 100,000 counts/second after the counting-loss correction.

Using SC, diffracted signals from a sample are

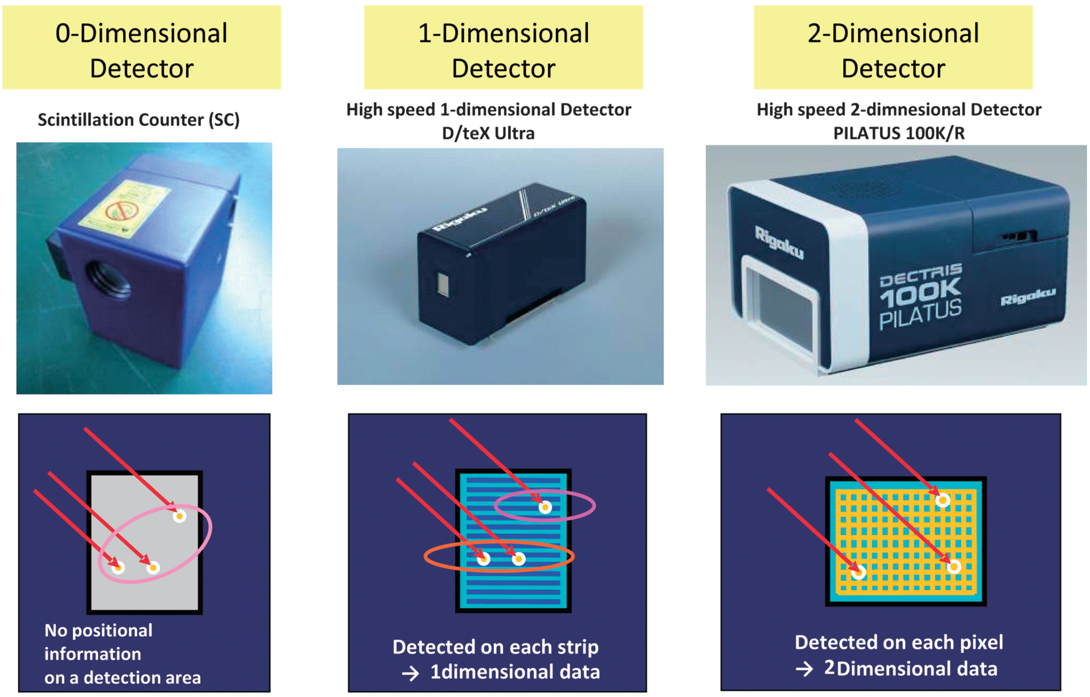

Fig. 1. Typical detectors for SmartLab system.

* Application Laboratories, Rigaku Corporation.

detected with wide detection area of a diameter around 1 inch. This type of detector, known as a 0D detector, does not have positional sensitivity, thus the signals for a given range of 2θ angles are summed up. In order to attain the angle resolution for 2θ, suitable receiving optics should be installed in front of the 0D detector, such as single or double receiving slits or a parallel slit analyzer (PSA), etc.

The wide detection area of SC is utilized by a PSA as a receiving element. By using PSA, it becomes possible to collect the signals spread and scattered on a sample surface without losing the angular resolution. In this lecture series, this situation was explained in the lectures on “Thin-film XRD method” in the 2nd lecture [6] and “In-plane XRD method” in the 4th lecture [7].

2.2. 1D Detector

It is getting easier to obtain solid-state semiconductor devices for X-ray detectors. By using this semiconductor device, detecting elements in a shape of strips are arranged in a one-dimensional array with narrow intervals. In recent years, this kind of solid-state semiconductor device has come to be utilized for the X-ray detector in a conventional X-ray diffractometer, and is usually referred to as a “high-speed 1D detector”. This detector is imbued with characteristics of high response and high energy discrimination, but the high speed measurement with this detector is actually enabled by the arranged strips on the detection area.

2.2.1. Principle of performing “high-speed measurement”

Figure 2 shows a measuring geometry for the Bragg-Brentano (BB) para-focusing method. Figure 2(a) shows a typical geometry for the measurement with a 0D detector (SC). The angle resolution is controlled by the combination of incident and receiving slits. Usually, narrow slits around 0.1 mm to 0.5 mm are employed for receiving slits, and this means, only a few parts of detection area of SC are utilized for this measurement. On the other hand, Figure 2(b) shows geometry of the BB method using a 1D detector (D/teX Ultra). In this geometry, narrow receiving slits which are employed in measurements with a 0D detector will be no longer used, but diffracted signals for different 2θ angles can be detected by strips on the detection area simultaneously. In the case of $\theta/2\theta$ scan, the intensity is integrated by a

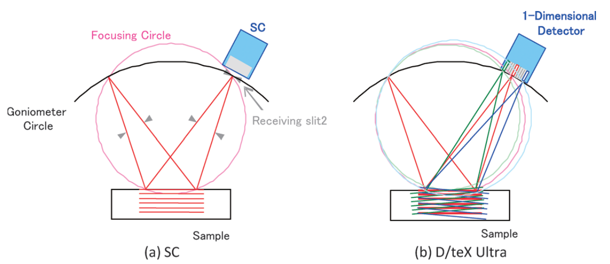

Fig. 2. Geometry of SC (0-dimensional detector) and 1-dimensional detector.

number of strips. This mode is referred to as “Time Delay Integration (TDI)” mode measurement. This is how “high-speed measurement” is enabled [8], [9].

This technique is effective for measurements by the para-focusing method for samples with textures of random orientation. For a sample with a texture of strong preferred orientation measured with a Parallel Beam (PB) geometry, this advantage of signal integration will be greatly reduced.

Signal integration cannot be restricted to the diffracted signals, but also is adapted inevitably to the signals of X-ray fluorescence from samples, which causes high background noises. For the solution of this problem, Rigaku’s 1D detector, “D/teX Ultra”, is equipped with a function called fluorescence-reduction mode. In this mode of measurement, the range of energy levels for signal integration can be controlled utilizing the energy discrimination of the semiconductor detector [2],[9].

2.2.2. 1D detector for thin film samples

Some notes and features using a 1D detector for a thin film sample are listed below.

- Conventional $2\theta/\omega$ measurement

As explained in the previous section, the advantage of signal integration (thus high-speed measurements) will be greatly reduced for samples with a texture of strong preferred orientation measured with a Parallel Beam (PB) geometry. If the divergence of the incident X-ray is larger, the integration effect increases. Angular resolution nevertheless, will be decreased.

By using this detector however, weak signals can be detected in a short time, which is advantageous for samples of small amount or minor phase detection [9], and also for the analysis of phase transitions in samples in a short time [8].

- Reciprocal space map measurement

A 1D detector has an advantage in Reciprocal Space Map (RSM) measurement in the field of high resolution thin film sample measurement. RSMs using conventional scintillation counters, are measured by the iterative motion of ω-step motions and $2\theta/\omega$ scans by changing scattering vector direction [10]. This measuring sequence cannot be directly applied to 1D detection. This is because a 1D detector in the TDI mode will integrate the scattering vector of different directions in the course of $2\theta/\omega$ scan. Instead, this problem will be cleared by iterative motion of ω-step and 2θ scans in TDI mode (not with $2\theta/\omega$ scan), and then, 2-dimensional RSM data can be obtained (Fig. 3). This measuring sequence with TDI mode is useful for RSM where data of a wide range of 2θ will be measured. Since the strip arrangement of detecting elements can cover a certain range of 2θ without scanning of 2θ (i.e., the detector is standing still), signals for a certain range of 2θ can be simultaneously collected by exposing an incident X-ray (with a fixed ω) for a short time. This mode of signal collection is called “Still mode” measurement (Fig. 4), and then, a high-speed

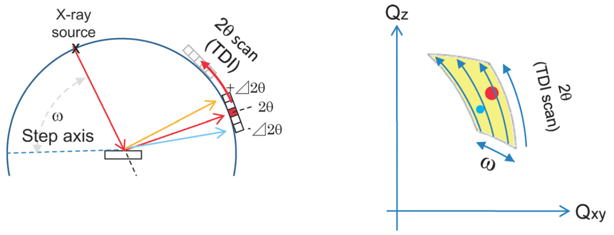

Fig. 3. Reciprocal Space map measurement by D/teX Ultra (ω step and 2θ scan) Left: Schematic illustration of goniometer movement, Right: Diagram of scanned area in reciprocal space.

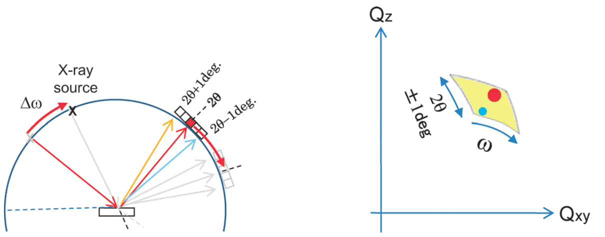

Fig. 4. Reciprocal Space map measurement by D/teX Ultra (2θ step and ω scan) Left: Schematic illustration of goniometer movement, Right: Diagram of scanned area in reciprocal space.

measurement is attained, due to the multiplication of the number of strips of detecting elements. In the SmartLab system, the two measurement modes above are installed.

Figure 3 shows ω-step 2θ-scan measurement for reciprocal space mapping using 1D detector. An ω angle is fixed for every step while 2θ scan. This method has an advantage for wide angle measurement.

Figure 4 shows 2θ-step ω-scan measurement for reciprocal space mapping using 1D detector. By this method, 2θ angle will be fixed while ω axis scanning. This method has advantage for small angle ($\Delta 2\theta < 2°$) measurement. This scanning mode is not a TDI mode, so the intensity will not integrated. Instead of integration, scattering vector of different angle can be obtained simultaneously. And by scanning of ω axis, reciprocal space map can be obtained. This method is also advantage of 1D detector.

For the RSM measurement, the geometry of incident/diffracted X-ray is also important. Figures 5 (a) and (b) show 2 different geometries for asymmetric RSM measurements. In general, low incident angle geometry (also called as Grazing-Incident geometry) is convenient for detecting weak signals from thin films. Thus, the geometry shown in Fig. 5(a) is generally employed for measurements for thin film samples, but the incident beam is spread over the sample surface due to the low incident angle, and consequently, the width of diffracted beam is wide.

Another geometry, i.e., low exit angle geometry (also called as Grazing-Exit geometry) is possible to be employed for measuring thin film samples (Fig. 5(b)), where a width of diffracted X-ray beam will be narrower than the one for the incident beam. For the RSM measurements using a 1D detector, the width of

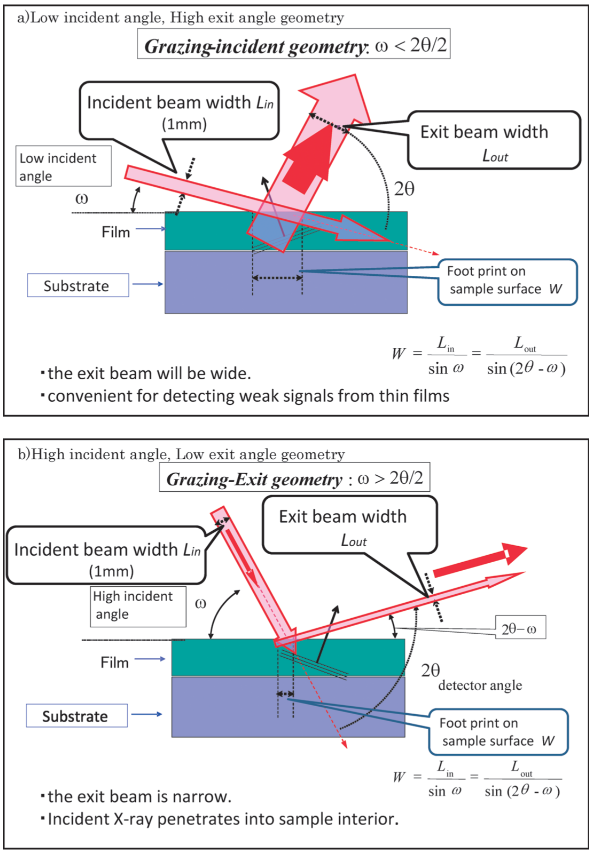

Fig. 5. 2 different geometries of asymmetric reciprocal space map measurement.

(a) Low angle incident, High angle exit geometry.

(b) High angle incident, Low angle exit geometry.

diffracted beam should be the same size as a strip of the detecting elements. The geometry shown in Fig. 5(b) should therefore be used for RSM measurements using 1D detector. Even if it is the symmetric-geometry, the width of incident beam should be controlled to be the same width as that of a detecting strip. A wider incident beam causes the reduction of resolution, and it often causes a streak in RSM data running along the trace of 2θ motion (thus, along the Ewald's circle).

- 0-dimensional mode

A 1D detector has many strips on the detection area, but by canceling out the 2θ information (positional sensitivity), this detector can be used as a 0D detector. This mode is called "0D mode" measurement. By using this mode, optical alignment and sample alignment can be carried out like using a scintillation counter. Also, with any kind of receiving optics, various measurements, such as high resolution Rocking Curve measurement (3rd lecture)[10] and X-ray reflectivity (5th lecture)[11], will be available. Selection of measuring modes can be performed in a manual control window or in measurement dialog boxes.

2.3. 2D Detector

There have been already equipped 2D detectors such as CCDs, Imaging Plates, X-ray films in a conventional

XRD system, but these detectors or recording media have some disadvantages like sensitivity, reading time, etc.

Recently, solid-state semiconductor devices such as X-ray detectors where detection pixels are arranged in 2 dimensional arrays on a detection area, have come to be commercially available. The SmartLab system can be equipped with "PILATUS 100K/R" as a high speed and quick read-time, single-photon counting 2D detector, which also has high dynamic range and high sensitivity. The details and features of this detector are described in articles[(3)–(5),(12)].

In comparison with a 2D gaseous detector, 2D solid-state semiconductor detectors have various advantages, including not only the high energy discrimination, but also the applicability of TDI mode like a 1D detector utilizing its potentiality of short readout time. In addition, due to the difference in finite thickness in the active sensing regions, solid-state semiconductor detectors have advantages (thin sensing region) over the gaseous detectors in the aspect of oblique incidence of X-ray to detectors.

2.3.1. Principle of performing "high-speed measurement"

Figure 6 shows a SmartLab system equipped with PILATUS 100K/R. The incident X-ray and diffracted X-rays are drawn as red lines. 2-dimensionally arranged detecting pixels can record data which can be obtained by data acquisition with the goniometric motion of 2θ scan and with that of almost equivalent to χ scan. An example of a data image measured by 2D detector is shown in Fig. 6(b). With this figure, it can be easily recognized that information of 2θ (i.e. information of d-spacing, thus those of lattice constants) and distribution of crystallite orientation (mosaic spreading) is recorded in a single shot of 2D image data, then, high speed measurement is attained.

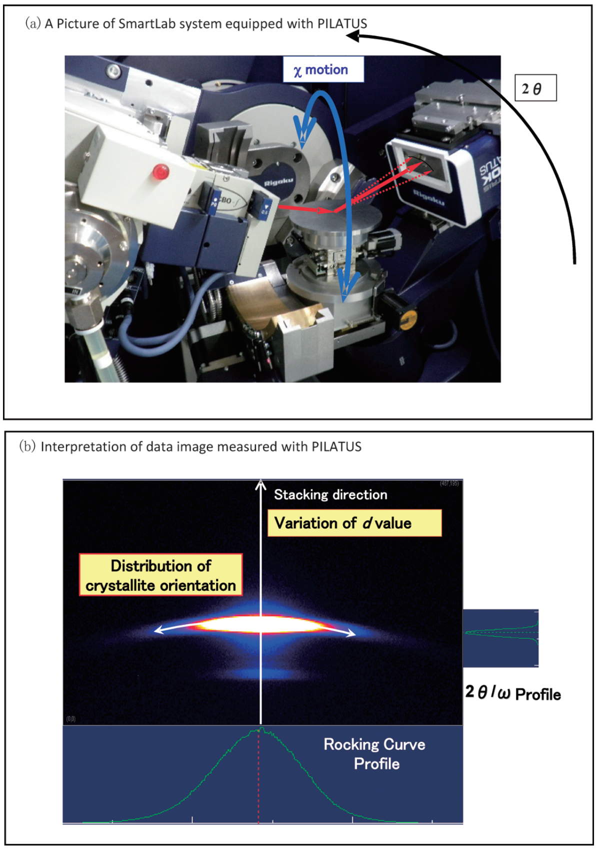

Fig. 6. (a) A picture of SmartLab system equipped with PILATUS 100K/R. (b) Interpretation of data image measured with PILATUS.

2.3.2. 2D detector for thin film sample measurement

In a previous paragraph, it is explained as "data acquisition with that of almost equivalent to χ scan". It should be noted that it is, expressly, not equivalent to the data acquisition with χ scan. As shown in Fig. 6(a), the diffracted beam which is detected at the position close to the edge of 2-dimensional detector enters the detector in a condition far away from the normal incidence to the detector surface; *i.e.*, the shape of the diffraction spots would be distorted due to the effect of oblique projection to the detecting plane.

Another factor which should be taken into account for the analysis of data detected close to the edge of 2D detectors is the interpretation of azimuthal directions, which is crucial for the analysis of epitaxial films. If the detection area is large enough, one might surmise that all of the diffraction signals both for $\theta/2\theta$ scans and In-plane scans can be obtained simultaneously, yet this is not correct. The diffraction condition should be satisfied with the sample rotation. This indicates that the diffraction condition should be satisfied with the sample rotation with ϕ axis for the diffraction signals observed with In-plane scans. Thus, a 2D data image with a single snapshot (or Still mode measurement) will collect signals with different azimuth information for the points of center and edge (right and left edge in figure) in the detection area. For the RSM measurements for single crystalline epitaxial films or substrates, RSM measurements of wide χ angle range covered with a big detection area detector are not appropriate. Instead, measurements with small χ steps, followed by the compilation data processing of these data in the data analysis software are effective. One may wonder whether the ω rotation will not be required as for the ϕ rotation of a sample. The answer is that it is required but it can be attained with the TDI mode scan. The PILATUS 100K/R can be covered the wide range of $2\theta/\omega$ angles by using TDI measurement mode like the 1D detector[(5),(13),(14)].

Cautions mentioned above are very important in measurements of epitaxial films or single crystalline samples, but almost negligible in those for thin film samples with textures of weak or no preferred orientations.

For the general measurement with 2D detector, nothing can be placed between sample and detector (Fig. 6(a)), so it is difficult to avoid scattering signals except

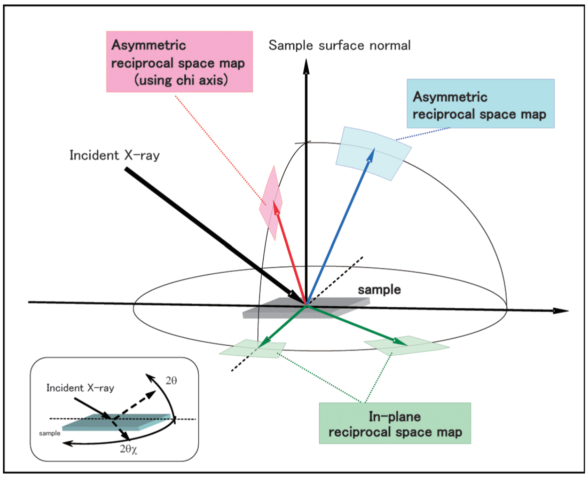

Fig. 7. Geometry of reciprocal space map.

from a sample itself, such as scattering from sample stages, or from dome covers or window materials of high temperature stages, etc.

The 2D detector will also work as a powerful tool of analysis via wide angle RSM measurements for epitaxial films with lattice distortions or tilting. High angular resolution will not be required for RSM measurements for these films, rather, data for the wide area in reciprocal space will be preferable. These requirements for measurements are complementary with the features of 2D detectors with TDI mode.

The geometries of RSM measurements are schematically shown in Fig. 7. The area marked with red lines is that for RSM measured by $2\theta/\omega$ scans combined with χ axis step-tilting (RSM with skew geometry for asymmetric lattice planes), which can be measured with 2D detector. The relative χ angle range will be ± 5 to 10 degrees at one $2\theta/\omega$ scan. Iterative motions of a goniometer as repeating χ steps and $2\theta/\omega$ scans, will lead to obtaining data for a wide area RSM.

As explained in the 6th lecture "Small angle X-ray scattering measurement"[15] and 7th lecture "Pole figure measurement"[16], 2D detectors have great advantages in these measurements, especially for GI-SAXS measurements[15],[17]–[19].

For the measurement using a 2D detector, it is generally required to set the incident X-ray beam as small as possible to be a point shape. However, this does not necessarily mean that a line-focused X-ray source should be changed to a point-focus source. For example, a combined set of narrow limit slits and PSCs (Parallel Slit Collimator) or collimators can be adopted for this purpose. Additionally, the SmartLab system can be equipped with a unique functional tool "CBO-*f*" as a converter from a line-shaped beam to a point-shaped beam in the incident optics.

Moreover, a line-shaped incident beam itself can be adopted for RSM measurements where higher signal intensities are preferred over the resolution. The data image with this optics configuration will be suffer from defocusing due to the umbrella effect, but the center of

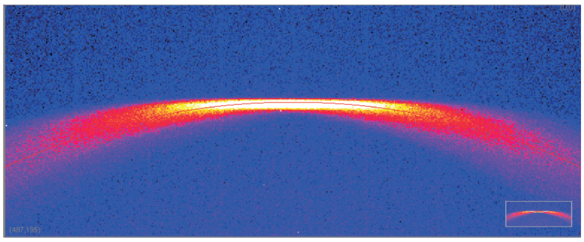

Fig. 8. Hi speed measurement with 2D detector (line focus).

the image will not be affected as much, as shown in Fig. 8.

3. Summary of this lecture course

With this, the eight lectures for basic measurement techniques of X-ray characterization of thin-film samples have been published. Titles for all lectures are listed as below.

I.	"Overview"	2008, Vol. 24, No. 1
II.	"Out-of-plane diffraction measurement"	2008, Vol. 25, No. 1
III.	"High resolution X-ray diffractometry"	2009, Vol. 25, No. 2
IV.	"In-plane XRD measurement"	2010, Vol. 26, No. 1
V.	"X-ray reflectivity measurement	2010, Vol. 26, No. 2
VI.	"Small angle X-ray scattering"	2011, Vol. 27, No. 1
VII.	"Pole figure measurement"	2011, Vol. 27, No. 2
VIII.	"Detectors and Series Summary"	this lecture

Recently, thin film materials are exhibiting remarkable evolution and progress. It may be required soon to make the updating revision for the list of measurement examples (1st lecture, Table 2)[1].

We have been asked many questions about measurement and analytical techniques from many users in the various fields. For the answers to each question, we have come to plan and edit this "X-ray Thin-film Measurement Techniques" lecture course. We hope these lectures will be helpful for many users, and may assist the thin film material research activity in the world.

References

(1) K. Inaba: *The Rigaku Journal (English version)*, **24** (2008), No. 1, 10–15.
(2) *The Rigaku Journal (English version)*, **24** (2008), No. 1, 30–32.
(3) Ch. Broennimann, E. F. Eikenberry, B. Henrich, R. Horisberger, G. Huelsen, E. Pohtl, B. Schmitt, C. Schulze-Briese, M. Suzuki, T. Tomizaki, H. Toyokawa and A. Wagner: *J. Synchrotron Rad.*, **13** (2006), 120–130.
(4) T. Taguchi, C. Brönnimann and E. F. Eikenberry: *Powder Diffraction*, **23** (2008), 101–105.
(5) P. Kraft, A. Bergamaschi, Ch. Broennimann, R. Dinapoli, E. F. Eikenberry, B. Henrich, I. Johamson, A. Mozzanica, C. M. Schlepütz, P. R. Willmatt and B. Schmitt: *J. Synchrotron Rad.*, **16** (2009), 368–375.
(6) T. Mitsunaga: *The Rigaku Journal (English version)*, **25** (2009),

No. 1, 7–12.

(7) S. Kobayashi: *The Rigaku Journal (English version)*, **26** (2010), No. 1, 3–11.

(8) A. Kishi: *The Rigaku Journal (English version)*, **25** (2009), No. 2, 9–13.

(9) Y. Namatame: *The Rigaku Journal (English version)*, **27** (2011), No. 1, 6–8.

(10) T. Konya: *The Rigaku Journal (English version)*, **25** (2009), No. 2, 1–8.

(11) M. Yasaka: *The Rigaku Journal (English version)*, **26** (2010), No. 2, 1–9.

(12) Y. F. Yano, T. Uruga, H. Tanida, H. Toyokawa, Y. Terada and H. Yamada: *Jour. Synchrotron Rad.*, **17** (2010), 511–516.

(13) T. Nakajima, T. Tsuchiya and T. Kumagai: *Cryst. Growth Design,* **10** (2010), 4861–4867.

(14) T. Nakajima, T. Tsuchiya and T. Kumagai: *Cryst. Eng. Comm.,* **13** (2011), 158–166.

(15) A. Ogi and K. Inaba: *The Rigaku Journal (English version)*, **27** (2011), No. 1, 1–5.

(16) K. Nagao and E. Kagami: *The Rigaku Journal (English version)*, **27** (2011), No. 2, 6–14.

(17) Y. Ito: *The Rigaku Journal (English version),* **25** (2009), No. 1, 1–6.

(18) Y. Ito, K. Omote, Y. Okazaki, Y. Nakayaka and H. Kawada: *Proc. of SPIE.*, **7638** (2010), 763810-1–763810-10.

(19) K. Omote, Y. Ito and Y. Okazaki: *Proc. of SPIE.,* **7638** (2010), 763811-1–763811-8.